

# Exogenous BMP-7 Facilitates the Recovery of Cardiac Function after Acute Myocardial Infarction through Counteracting TGF- $\beta$ 1 Signaling Pathway

Yalei Jin,<sup>1</sup> Xinyao Cheng,<sup>2</sup> Jinping Lu<sup>1</sup> and Xia Li<sup>1</sup>

<sup>1</sup>Department of Geriatrics, Zhongnan Hospital, Wuhan University, Wuhan, Hubei, China

<sup>2</sup>Department of Echocardiography, Zhongnan Hospital, Wuhan University, Wuhan, Hubei, China

Myocardial fibrosis after acute myocardial infarction (AMI) is one of the main causes of myocardial remodeling and heart function abnormalities. Bone morphogenetic protein-7 (BMP-7) has been reported to play essential roles in anti-fibrosis. In this study, we demonstrated the role of exogenous BMP-7 on myocardial fibrosis and heart function recovery after AMI. A rat model of AMI was established via ligation of the left anterior descending coronary artery (LAD). Twenty rats were grouped into sham group which underwent chest open operation, but did not receive LAD ligation. Another 40 rats underwent LAD ligation were randomly grouped into saline-treated group (n = 20) and BMP-7-treated group (n = 20) which received saline treatment or exogenous BMP-7 treatment for 14 days, respectively. Two weeks after LAD ligation, the survival rate of BMP-7-treated AMI group was significantly improved compared to the saline group. Moreover, the cardiac function was preserved as shown by echocardiography examination, and the infarcted size was limited upon BMP-7 treatment. In addition, we investigated the role of TGF- $\beta$ 1 signaling pathway in BMP-7-mediated cardioprotective effects by analyzing the expression levels of TGF- $\beta$ 1, Smad 2 and Smad 3 in the infarct zone, border zone, and non-infarct zone. Western blot and quantitative PCR results suggested that BMP-7 attenuated myocardial fibrosis through counteracting TGF- $\beta$ 1 signaling pathway, thereby exerting cardioprotective effects. In conclusion, our data provide a potential therapeutic direction for preserving cardiac function and improving prognosis of AMI patients.

**Keywords:** AMI; BMP7; myocardial fibrosis; Smad; TGF- $\beta$ 1

Tohoku J. Exp. Med., 2018 January, 244 (1), 1-6. © 2018 Tohoku University Medical Press

## Introduction

Acute myocardial infarction (AMI) is becoming the leading cause of cardiac death worldwide (Mozaffarian et al. 2016). Myocardial remodeling and heart function abnormalities after AMI affect patients' prognosis and living quality (Burchfield et al. 2013). AMI results in scar formation, which can enhance the local contractility and prevent the heart from burst. However, over-deposition of collagens and fibrosis contributes to ventricular enlargement, subsequently impairs the myocardial contract and dilate abilities, leading to heart function deficiency and heart failure (Uusimaa et al. 1997; Towbin 2007; Zeisberg et al. 2007). Myocardial remodeling and collagen deposition is a long term pathophysiological change after AMI. Unfortunately, little drug was known to prevent myocardial fibrosis (Reichert et al. 2016). Lacking preventive therapy for myocardial remodeling in AMI patients highlights the urgent demand for developing novel drugs, which will be invaluable in delaying heart structural damage.

The transforming growth factor  $\beta$  (TGF- $\beta$ ) cytokine superfamily is composed of the prototypic TGF- $\beta$ s and bone morphogenetic proteins (BMPs) (Massague 2012). TGF- $\beta$ 1 signaling participates in various physiological and pathological processes including embryonic development, tissue differentiation, cell proliferation, inflammation, angiogenesis, tumorigenesis as well as fibrosis (Wu et al. 2016; Lei et al. 2017; Li et al. 2017; Tang et al. 2017; Wang et al. 2017; Yamazaki et al. 2017; Yang et al. 2017). Through regulating Smad2/3, TGF- $\beta$ 1 modulates the transcription and expression of several fibrosis-associated genes, thereby enhancing the synthesis of collagen and fibronectin (Dooley et al. 2008; Yan and Chen 2011; Massague 2012). Overstimulation of TGF- $\beta$  signaling pathway contributes to aberrant deposition of extracellular matrix (ECM), leading to the pathological heart remodeling after AMI (Dobaczewski et al. 2011). Intriguingly, it has been reported that BMP-7, an important member of BMPs subfamily, can counteract TGF- $\beta$ 1-induced ECM accumulation in several models. In other words, BMP-7 may be

Received July 28, 2017; revised and accepted December 4, 2017. Published online December 27, 2017; doi: 10.1620/tjem.244.1.

Correspondence: Yalei Jin, Department of Geriatrics, Zhongnan Hospital, Wuhan University, #169 Donghu Road, Wuhan 430071, Hubei, China.

e-mail: jinyalei\_zhongnan@163.com

potential in down-regulating the interstitial fibrosis, including both kidney fibrosis and heart fibrosis (Zeisberg et al. 2003; Weiskirchen and Meurer 2013).

In the present study, we investigated whether recombinant BMP-7 administration can improve the overall survival and reduce the heart infarction size in a rat AMI model. Using this model, we firstly tested the effect of recombinant BMP-7 on heart functions, and further assessed the fibrosis level as well as corresponding protein biomarkers in the heart tissues. Finally, whether BMP-7 affects the fibrosis accumulation through modulating TGF- $\beta$ 1 signaling pathway was verified.

## Materials and Methods

### *Rat model of AMI and treatment protocol*

Adult male Sprague-Dawley (SD) rats weighing  $250 \pm 20$  g obtained from the Laboratory Animal Center of Wuhan University were used in this study. The study was approved by the Animal Ethics Committee of the Medical School of Wuhan University and conducted in accordance with the guidelines from the National Institutes of Health guide for the care and use of Laboratory animals. All animals received humane care, and all efforts were made to minimize animal suffering. All surgery was performed under sodium pentobarbital anesthesia. In brief, animals were anesthetized, and the chest was opened followed by LAD (left anterior descending artery)-ligation. The rats in sham group underwent same anesthetization and chest open operation, but did not receive LAD ligation. The LAD ligation position was 1-2 mm distal to the line between left border of the pulmonary conus and right border of left atrial appendage. After surgery, LAD-ligated rats were randomly assigned to two groups (saline group, and BMP-7 treatment group). For the BMP-7 treatment group, recombinant murine BMP-7 (5666-BP, R&D Systems), which is 100% in sequence identity to the rat BMP-7, was administered intraperitoneally for 2 weeks ( $5 \mu\text{g}/\text{kg}/\text{day}$ ); whereas rats in sham group and saline group were treated with saline.

### *Echocardiography measurement*

After 2 weeks' treatment, the heart function was evaluated using a Siemens Acuson™ SC2000 high-frequency ultrasound system (Siemens, Inc., Berlin, Germany). A Two-dimensional echocardiographic measurement was obtained after rat anesthetization. The left ventricular end-diastolic diameter (LVEDD), left ventricular end-systolic diameter (LVESD), left ventricular ejection fraction (LVEF), and left ventricular fractional shortening (LVFS) were all measured and calculated from the M-mode tracing.

### *Evaluation of myocardial infarction size*

Following euthanasia, hearts were collected. After stored at  $-20^{\circ}\text{C}$  for 20 min, the hearts were cut into 2-mm slices across the long axis, incubated with 2% triphenyl-tetrazolium chloride (Sigma, St Louis, USA) at  $37^{\circ}\text{C}$  for 30 min in dark, and then fixed by 10% paraformaldehyde overnight. The infarcted site was pale white visually, whereas the normal tissue appeared brick-red. All tissue slices were imaged, and infarcted size was calculated using Image-Pro Plus 6.0 software (Media Cybernetics, Silver Spring, USA).

### *Fibrosis evaluation*

The extent of fibrosis was measured by Masson staining. Briefly, after heart tissues were fixed and embedded in paraffin, 4- $\mu\text{m}$  sections were cut and stained with hematoxylin/eosin and Masson's trichrome, respectively. Each section was imaged by microscopy (Nikon, Japan). The ratio of fibrotic area to the total area of connective and myocardial tissue was calculated using Image-Pro Plus 6.0 software.

### *Quantitative real-time PCR (qRT-PCR) analysis*

The relative gene transcription was analyzed by qRT-PCR. Total RNA was isolated from left ventricular tissues with Trizol reagent (Invitrogen, CA, USA) following manufacturer's instructions. Concentration of total RNA was estimated, and the qRT-PCR was conducted as described by others (Liu et al. 2016). The primer sequences are shown in Table 1. Gene expression levels were normalized to glyceraldehyde-3-phosphate dehydrogenase (GAPDH). Expression levels of each mRNA were measured in duplicate with five independent experiments.

### *Western blot analysis*

Western blot was used to evaluate the protein expression levels. Briefly, 20  $\mu\text{g}$  of protein lysates was electrophoresed by 10% SDS-PAGE and transferred onto polyvinylidene difluoride (PVDF) membranes (Bio-Rad, CA, USA). The primary antibodies included rabbit polyclonal anti-TGF- $\beta$ 1 (Santa Cruz, CA, USA), rabbit polyclonal anti-SMAD2/3 (Abcam, Cambridge, United Kingdom), and mouse monoclonal anti-GAPDH antibodies (ZSGB-BIO Co., China). After incubated with appropriate secondary antibodies, membranes were immunodetected with ECL Advance Western Blotting Detection Kit (GE Healthcare, Germany). The immunoreactivity was expressed as optical density of the sample dots normalized to that of GAPDH. Samples from 3-6 subjects per group were tested in two independent experiments.

Table 1. List of Primers in qRT-PCR.

Genes	Forward	Reverse
TGF- $\beta$ 1	5'-TGCTTCAGCTCCACAGAGAA-3'	5'-TGGTTGTAGAGGGCAAGGAC-3'
Smad2	5'-AGTGTTTGCCGAGTGCCTAA-3'	5'-GCCTCAAAAACCTGGTTAAC-3'
Smad3	5'-GGCAGGATGTTTCCAGCTA-3'	5'-GCAGTCCACAGACCATGTCA-3'
Collagen1	5'-TCCTGGCAATCGTGGTTCAA-3'	5'-ACCAGCTGGGCCAACATTTTC-3'
Collagen3	5'-TGGACAGATGCTGGTGCTGAG-3'	5'-GAAGGCCAGCTGTACATCAAGGA-3'
Fibronectin	5'-GCACATGTCTCGGAATGGA-3'	5'-ACACGTGCAGGAGCAAATGG-3'
GAPDH	5'-GGCACAGTCAAGGCTGAGAATG-3'	5'-ATGGTGGTGAAGACGCCAGTA-3'

### Statistical analysis

GraphPad Prism 5 software was used for statistical analysis and for generating graphs. All values were described as mean  $\pm$  S.D. One-way ANOVA test was utilized to compare the statistical differences among groups, and Tukey's test was used for post hoc analyses. A Kaplan-Meier survival analysis was used to evaluate the overall survival rates of the rats. A P-value  $< 0.05$  was considered statistically significant.

## Results

### Recombinant BMP-7 improves overall survival rate in rats with AMI

By LAD ligation, we developed a rat AMI model to explore the effect of BMP-7 on the heart remodeling and fibrosis. After 2 weeks of BMP-7 treatment, the overall survival rate was determined. All rats in the sham group, which were not subjected to LAD ligation, survived after 14 days; while nearly half of the rats in the saline group died within the first week after operation (Fig. 1A). Heart failure seemed to be the main cause of death. Importantly, the survival rate of rats in the BMP-7 treatment group was

better than that of the saline group (70% and 45%, respectively). Nevertheless, although significant difference was observed by comparing three groups (sham, saline, BMP7; log-rank  $p = 0.0006$ ) and the trend indicated improved outcomes in the rats upon BMP-7 administration, it was not statistically significant between the saline and BMP7 groups ( $p = 0.1221$ ). The heart weight/body weight (HW/BW) ratio was also evaluated after the rats were euthanized, which revealed that the ratio was significantly lower in the BMP-7 treatment group compared with the saline and sham groups (Fig. 1B).

### Recombinant BMP-7 improves echocardiographic performance in rats with AMI

Two weeks after the induction of AMI, two-dimensional echocardiography was performed to detect the heart function changes. As revealed in Fig. 2, after AMI operation, LVEDD and LVESD were increased, while LVFS and LVEF were decreased compared to the parameters in sham group, indicating an impaired myocardial contractility. Moreover, BMP-7 treatment significantly down-regulated

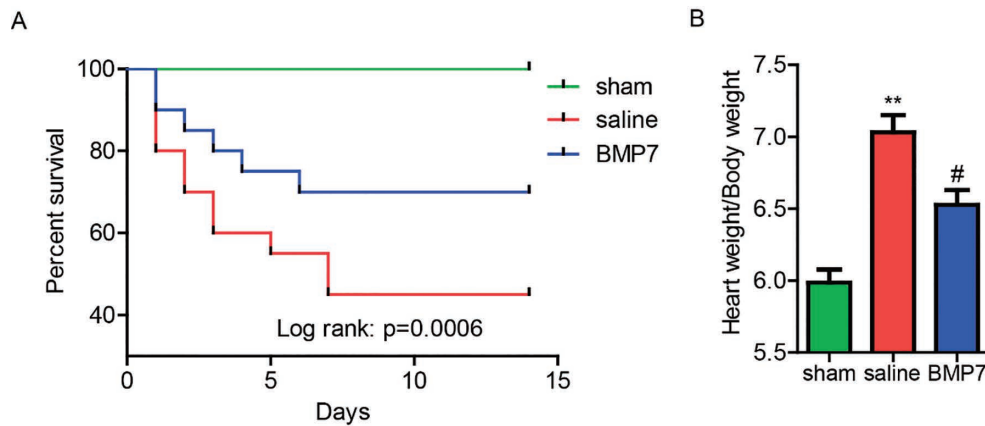


Fig. 1. Recombinant BMP-7 improves overall survival rate and decreases the heart/body weight ratio in a rat AMI model.

(A) Kaplan-Meier analysis indicated the survival rates of rats after AMI.

Green line, survival rate of the sham group ( $n = 20$ ); Red line, survival rate of the saline group ( $n = 20$ ); Blue line, survival rate of the BMP-7 treated group ( $n = 20$ ). (B) Analysis of the heart weight/body weight ratio, data were expressed as mean  $\pm$  SD. \*\* $P < 0.01$  versus sham group, # $P < 0.05$  versus saline group.

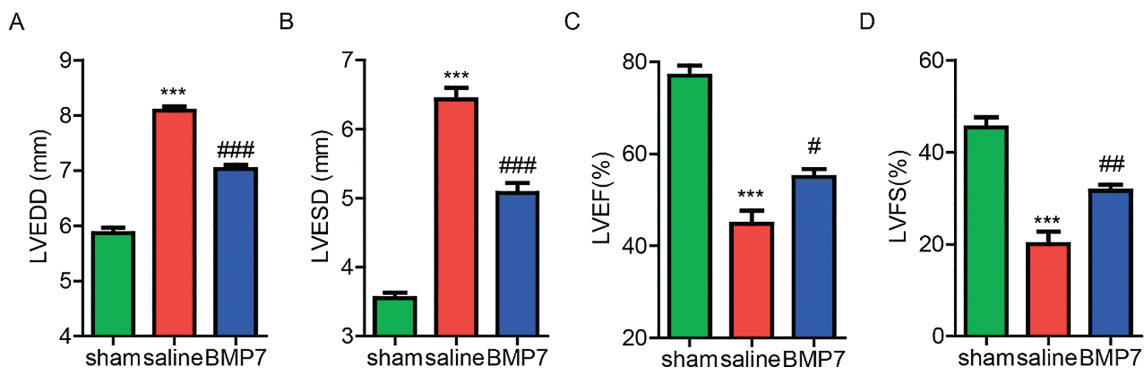


Fig. 2. Recombinant BMP-7 improves the cardiac performance in the rat AMI model.

The echocardiographic analyses toward LVEDD (A), LVESD (B), LVEF (C), and LVFS (D) were conducted after 2-week treatment, respectively. Data are expressed as mean  $\pm$  SD. \*\*\* $P < 0.001$  versus sham group, # $P < 0.05$  versus saline group, ### $P < 0.01$  versus saline group, #### $P < 0.001$  versus saline group.

LVEDD and LVESD; on the other hand, LVFS and LVEF were up-regulated compared with the saline group. The results above implicated an improvement of cardiac functions in AMI rats after BMP-7 treatment.

#### Recombinant BMP-7 inhibits myocardial fibrosis

BMP-7 has been reported to be an antagonist of TGF- $\beta$ 1 signaling pathway and can reduce the fibrosis level of certain organs (Zeisberg et al. 2003; Weiskirchen and Meurer 2013). We set to illustrate whether recombinant BMP-7 improves the heart function by decreasing myocardial fibrosis in the rat AMI model. H&E and Masson's trichrome staining were performed to detect the pathological changes and fibrosis in the myocardial tissue, respectively. Compared to the saline group, the infarct size (Fig. 3A) and interstitial fibrosis (Fig. 3B) were both significantly decreased in BMP-7 treatment group, indicating a potential anti-fibrotic effect of BMP-7 in AMI.

Furthermore, qRT-PCR experiment was performed to determine the expression of certain fibrosis markers including collagen1, collagen3 and fibronectin in the infarct zone (IZ), border zone (BZ), non-infarct zone (NIZ), respectively. In accordance with previous study (Hou et al. 2015), maximum expression of fibrosis markers were detected in the infarct zone while minimum expression in the non-infarct zone (Fig. 3C-E). Additionally, expression levels of fibrosis markers were decreased in all zones from BMP-7 treatment group, compared with saline group.

#### Recombinant BMP-7 treatment attenuates TGF- $\beta$ 1 signaling

To investigate whether BMP-7 induced inhibition of myocardial fibrosis by counteracting the TGF- $\beta$ 1 signaling pathway, we tested the expression of several effectors in TGF- $\beta$ 1 signaling pathways through western blot and qRT-PCR. The mRNA level of TGF- $\beta$ 1 was upregulated in the saline groups compared with the sham group in the infarct, border and non-infarct zones (Fig. 4A). Besides, its mRNA level was downregulated in the BMP-7 treatment group compared with the saline group. As two of the most important downstream effectors of TGF- $\beta$ 1, Smad2 and Smad3 showed similar alterations upon BMP-7 treatment (Fig. 4B, C). Accordingly, the protein expression changes showed a similar tendency as revealed by immunoblotting (Fig. 4D).

### Discussion

Accumulated evidence suggested that BMP-7 signaling was beneficial to resolve established organ damage, especially renal and hepatic progressive fibrosis (Wang et al. 2006; Sugimoto et al. 2007; Zeisberg and Kalluri 2008). Of note, small peptide agonists of BMP-7 receptors have been developed to inhibit kidney inflammation, tissue damage, and fibrosis (Sugimoto et al. 2007). However, to date, no small regulator targeting the myocardial fibrosis was reported. BMP-7 has been reported to be involved in cardiac myogenesis of chick embryo, and BMP signaling pathways are functional in cardiac myocytes from mice, rats, and humans (Schultheiss et al. 1997; Wu et al. 2014). To

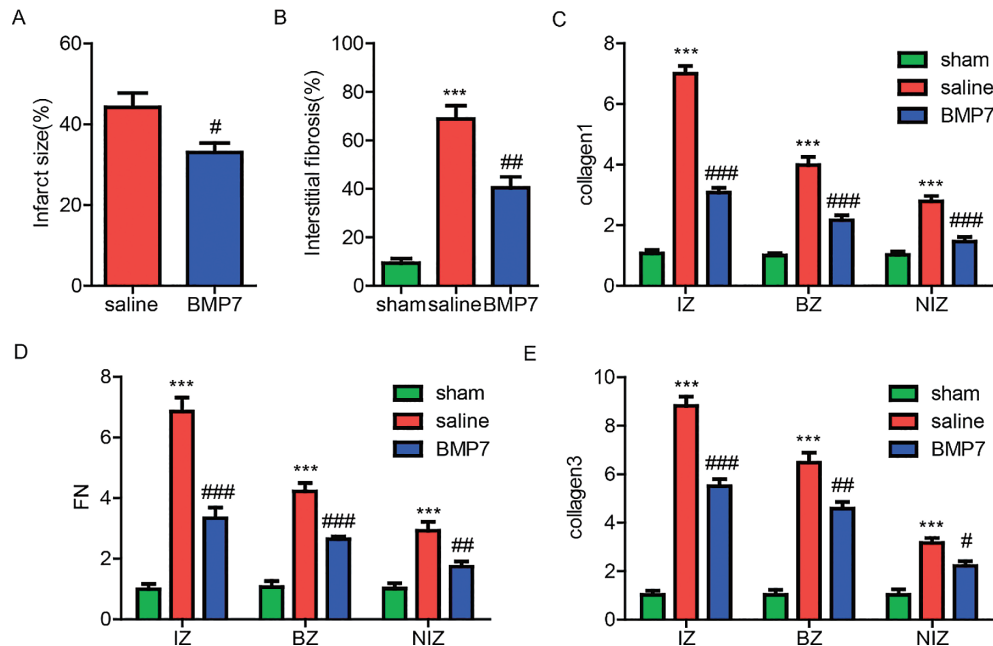


Fig. 3. Myocardial fibrosis level and infarct size are decreased upon BMP-7 treatment in the rat AMI model.

(A) Percent infarct size of saline group and BMP-7 treated group. (B) Interstitial fibrosis of sham group, saline group and BMP-7 treated group. (C-E) Relative mRNA expression levels of several fibrosis markers in infarct zone (IZ), border zone (BZ) and non-infarct zone (NIZ). (C) Relative mRNA expression levels of collagen1. (D) Relative mRNA expression levels of fibronectin (FN). (E) Relative mRNA expression levels of collagen3. Data were presented as mean  $\pm$  SD. \*\*\*P < 0.001 versus sham group, #P < 0.05 versus saline group, ##P < 0.01 versus saline group, ###P < 0.001 versus saline group.

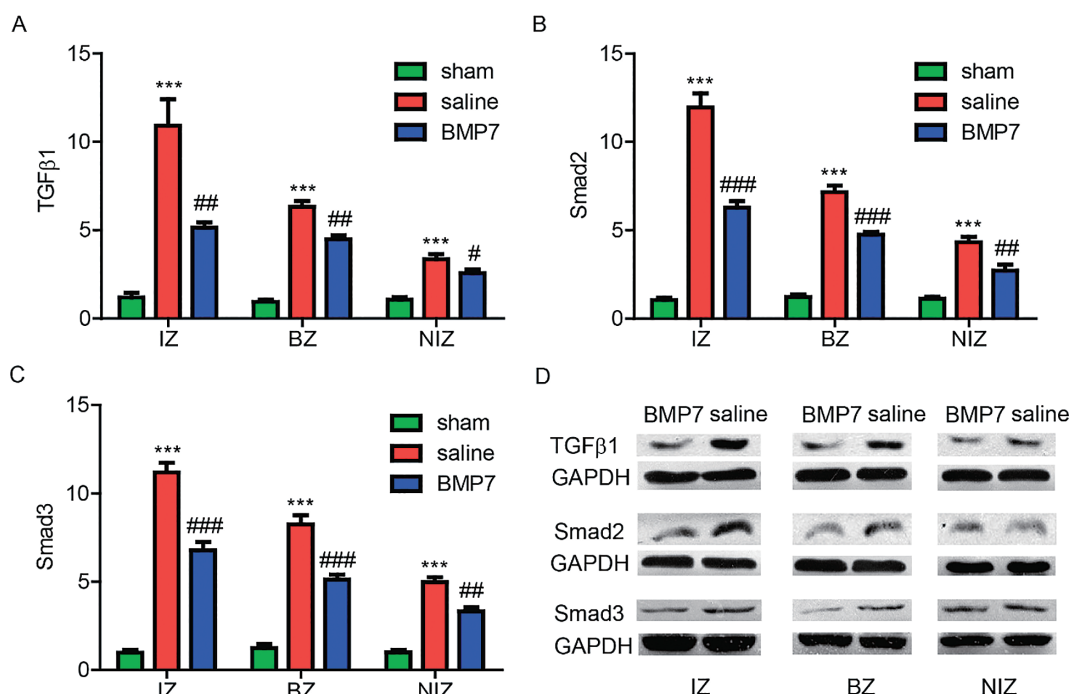


Fig. 4. Recombinant BMP-7 treatment attenuates TGF- $\beta$ 1 signaling in different areas of the left ventricle. (A)-(C) Relative mRNA expression levels of TGF- $\beta$ 1 signaling participants in infarct zone (IZ), border zone (BZ) and non-infarct zone (NIZ). (A) Relative mRNA expression levels of TGF- $\beta$ 1. (B) Relative mRNA expression levels of Smad2. (C) Relative mRNA expression levels of Smad3. (D) Western blot analysis of protein expression levels in infarct zone (IZ), border zone (BZ) and non-infarct zone (NIZ). Data were presented as mean  $\pm$  SD. \*\*\*P < 0.001 versus sham group, #P < 0.05 versus saline group, ##P < 0.01 versus saline group, ###P < 0.001 versus saline group.

our knowledge, whether exogenous administration of recombinant BMP-7 plays a role in regulating myocardial fibrosis and facilitating heart functional recovery after AMI is still unknown. Our research found that administration of recombinant BMP-7 improved the overall survival rate and benefit heart functional recovery in a rat AMI model, suggesting the promising role of BMP-7 on the treatment of AMI.

BMP-7 and TGF- $\beta$ 1 belong to the same cytokine superfamily, whereas each exhibits a unique signaling pathway through specific Smad proteins. During the process of pathological heart remodeling induced by AMI, TGF- $\beta$ 1 is a potent mediator of myocardial fibrosis and hypertrophy. Conversely, BMP-7 acts as an anti-fibrotic cytokine in experimental models of pathological organ fibrosis (Massague 2012). In support of a protective effect against cardiac pathological remodeling, treatment with recombinant BMP-7 in a rat AMI model counteracted the TGF- $\beta$ 1 signaling pathway. Therefore, recombinant BMP-7 may prevent the development of myocardial fibrosis, and subsequently improve the cardiac functions.

In summary, our findings indicate that recombinant BMP-7 exerts cardioprotective effects by attenuating myocardial fibrosis through counteracting TGF- $\beta$ 1 signaling pathway in the rat AMI model. The value of recombinant BMP-7 on regulating myocardial fibrosis and improving the overall survival deserves further attention.

## Acknowledgments

This work was supported by grants from the Natural Science Foundation of Hubei Province (grant number 2015CFB650).

## Conflict of Interest

The authors declare no conflict of interest.

## References

- Burchfield, J.S., Xie, M. & Hill, J.A. (2013) Pathological ventricular remodeling: mechanisms: part 1 of 2. *Circulation*, **128**, 388-400.
- Dobaczewski, M., Chen, W. & Frangogiannis, N.G. (2011) Transforming growth factor (TGF)- $\beta$  signaling in cardiac remodeling. *J. Mol. Cell. Cardiol.*, **51**, 600-606.
- Dooley, S., Hamzavi, J., Ciucan, L., Godoy, P., Ilkavets, I., Ehnert, S., Ueberham, E., Gebhardt, R., Kanzler, S., Geier, A., Breitkopf, K., Weng, H. & Mertens, P.R. (2008) Hepatocyte-specific Smad7 expression attenuates TGF-beta-mediated fibrogenesis and protects against liver damage. *Gastroenterology*, **135**, 642-659.
- Hou, J., Wang, L., Hou, J., Guo, T., Xing, Y., Zheng, S., Zhou, C., Huang, H., Long, H., Zhong, T., Wu, Q., Wang, J. & Wang, T. (2015) Peroxisome proliferator-activated receptor gamma promotes mesenchymal stem cells to express connexin43 via the inhibition of TGF- $\beta$ 1/smads signaling in a rat model of myocardial infarction. *Stem Cell Rev.*, **11**, 885-899.
- Lei, K., Liang, X., Gao, Y., Xu, B., Xu, Y., Li, Y., Tao, Y., Shi, W. & Liu, J. (2017) Lnc-ATB contributes to gastric cancer growth through a MiR-141-3p/TGF $\beta$ 2 feedback loop. *Biochem. Biophys. Res. Commun.*, **484**, 514-521.
- Li, Y., Zhu, H., Wei, X., Li, H., Yu, Z., Zhang, H. & Liu, W. (2017)

- LPS induces HUVEC angiogenesis in vitro through miR-146a-mediated TGF-beta1 inhibition. *Am. J. Transl. Res.*, **9**, 591-600.
- Liu, H., Zhang, Q., Li, K., Gong, Z., Liu, Z., Xu, Y., Swaney, M.H., Xiao, K. & Chen, Y. (2016) Prognostic significance of USP33 in advanced colorectal cancer patients: new insights into  $\beta$ -arrestin-dependent ERK signaling. *Oncotarget*, **7**, 81223-81240.
- Massague, J. (2012) TGF $\beta$  signalling in context. *Nat. Rev. Mol. Cell Biol.*, **13**, 616-630.
- Mozaffarian, D., Benjamin, E.J., Go, A.S., Arnett, D.K., Blaha, M.J., Cushman, M., Das, S.R., de Ferranti, S., Despres, J.P., Fullerton, H.J., Howard, V.J., Huffman, M.D., Isasi, C.R., Jimenez, M.C., Judd, S.E., et al. (2016) Heart disease and stroke statistics-2016 update: a report from the American heart association. *Circulation*, **133**, e38-360.
- Reichert, K., Pereira do Carmo, H.R., Galluce Torina, A., Diogenes de Carvalho, D., Sposito, A.C., de Souza Vilarinho, K.A., da Mota Silveira-Filho, L., Martins de Oliveira, P.P. & Petrucci, O. (2016) Atorvastatin improves ventricular remodeling after myocardial infarction by interfering with collagen metabolism. *PLoS One*, **11**, e0166845.
- Schultheiss, T.M., Burch, J.B. & Lassar, A.B. (1997) A role for bone morphogenetic proteins in the induction of cardiac myogenesis. *Genes Dev.*, **11**, 451-462.
- Sugimoto, H., Yang, C., LeBleu, V.S., Soubasakos, M.A., Giraldo, M., Zeisberg, M. & Kalluri, R. (2007) BMP-7 functions as a novel hormone to facilitate liver regeneration. *FASEB J.*, **21**, 256-264.
- Tang, P.M., Zhou, S., Meng, X.M., Wang, Q.M., Li, C.J., Lian, G.Y., Huang, X.R., Tang, Y.J., Guan, X.Y., Yan, B.P., To, K.F. & Lan, H.Y. (2017) Smad3 promotes cancer progression by inhibiting E4BP4-mediated NK cell development. *Nat. Commun.*, **8**, 14677.
- Towbin, J.A. (2007) Scarring in the heart: a reversible phenomenon? *N. Engl. J. Med.*, **357**, 1767-1768.
- Uusimaa, P., Risteli, J., Niemela, M., Lumme, J., Ikaheimo, M., Jounela, A. & Peuhkurinen, K. (1997) Collagen scar formation after acute myocardial infarction: relationships to infarct size, left ventricular function, and coronary artery patency. *Circulation*, **96**, 2565-2572.
- Wang, S., de Caestecker, M., Kopp, J., Mitu, G., Lapage, J. & Hirschberg, R. (2006) Renal bone morphogenetic protein-7 protects against diabetic nephropathy. *J. Am. Soc. Nephrol.*, **17**, 2504-2512.
- Wang, Z., Han, Z., Tao, J., Wang, J., Liu, X., Zhou, W., Xu, Z., Zhao, C., Wang, Z., Tan, R. & Gu, M. (2017) Role of endothelial-to-mesenchymal transition induced by TGF- $\beta$ 1 in transplant kidney interstitial fibrosis. *J. Cell. Mol. Med.*, **21**, 2359-2369.
- Weiskirchen, R. & Meurer, S.K. (2013) BMP-7 counteracting TGF-beta1 activities in organ fibrosis. *Front. Biosci. (Landmark Ed)*, **18**, 1407-1434.
- Wu, M., Chen, G. & Li, Y.P. (2016) TGF- $\beta$  and BMP signaling in osteoblast, skeletal development, and bone formation, homeostasis and disease. *Bone Res.*, **4**, 16009.
- Wu, X., Sagave, J., Rutkovskiy, A., Haugen, F., Baysa, A., Nygard, S., Czibik, G., Dahl, C.P., Gullestad, L., Vaage, J. & Valen, G. (2014) Expression of bone morphogenetic protein 4 and its receptors in the remodeling heart. *Life Sci.*, **97**, 145-154.
- Yamazaki, T., Nalbandian, A., Uchida, Y., Li, W., Arnold, T.D., Kubota, Y., Yamamoto, S., Ema, M. & Mukoyama, Y.S. (2017) Tissue myeloid progenitors differentiate into pericytes through TGF- $\beta$  signaling in developing skin vasculature. *Cell Rep.*, **18**, 2991-3004.
- Yan, X. & Chen, Y.G. (2011) Smad7: not only a regulator, but also a cross-talk mediator of TGF- $\beta$  signalling. *Biochem. J.*, **434**, 1-10.
- Yang, K.L., Chang, W.T., Hong, M.Y., Hung, K.C. & Chuang, C.C. (2017) Prevention of TGF- $\beta$ -induced early liver fibrosis by a maleic acid derivative anti-oxidant through suppression of ROS, inflammation and hepatic stellate cells activation. *PLoS One*, **12**, e0174008.
- Zeisberg, E.M., Tarnavski, O., Zeisberg, M., Dorfman, A.L., McMullen, J.R., Gustafsson, E., Chandraker, A., Yuan, X., Pu, W.T., Roberts, A.B., Neilson, E.G., Sayegh, M.H., Izumo, S. & Kalluri, R. (2007) Endothelial-to-mesenchymal transition contributes to cardiac fibrosis. *Nat. Med.*, **13**, 952-961.
- Zeisberg, M., Hanai, J., Sugimoto, H., Mammoto, T., Charytan, D., Strutz, F. & Kalluri, R. (2003) BMP-7 counteracts TGF- $\beta$ 1-induced epithelial-to-mesenchymal transition and reverses chronic renal injury. *Nat. Med.*, **9**, 964-968.
- Zeisberg, M. & Kalluri, R. (2008) Reversal of experimental renal fibrosis by BMP7 provides insights into novel therapeutic strategies for chronic kidney disease. *Pediatr. Nephrol.*, **23**, 1395-1398.